Membrane-Forming Properties of Gemini Lipids Possessing Aromatic Backbone between the Hydrocarbon Chains and the Cationic Headgroup

Santanu Bhattacharya*,†,‡ and Avinash Bajaj†

Department of Organic Chemistry, Indian Institute of Science, Bangalore 560 012, India, and Chemical Biology Unit of JNCASR, Bangalore 560 064, India

Received: June 27, 2007; In Final Form: September 4, 2007

Membrane-forming properties of five new gemini cationic lipids possessing an aromatic backbone between the headgroup and hydrocarbon chains have been presented. These gemini lipids differ by the number of polymethylene units [$-(CH_2)_n-$] between the cationic ammonium $-[N^+(CH_3)_2]-$ headgroups. The membrane-forming properties of these gemini lipids have been studied in detail by transmission electron microscopy (TEM), dynamic light scattering (DLS), X-ray diffraction (XRD), high-sensitivity differential scanning calorimetry (DSC), Paldan fluorescence studies, and UV−vis absorption spectroscopy. The electron micrographs and dynamic light scattering of their aqueous suspensions confirmed the formation of vesicular-type aggregates. The vesicle sizes and morphologies were found to depend strongly on the *n*-value of the spacer. Information on the thermotropic and hydration properties of the resulting vesicles was obtained from differential scanning calorimetry and temperature-dependent Paldan fluorescence studies, respectively. Examination of the thermotropic phase-transition properties of the lipid aggregates revealed interesting features of these lipids, which were found to depend on the length of the spacer chain. Paldan fluorescence studies indicate that the membranes of the gemini lipids are less hydrated as compared to that of the monomeric counterpart in their solid-gel state. In contrast in their fluid, liquid-crystalline phase, the hydration of gemini lipid aggregates was found to depend strongly on the length of the spacer. UV−vis absorption studies suggest an apparent H-type aggregate formation in the gemini lipid membranes in the gel states. In fluid state of the lipid membranes, H-aggregate formation was found to be enhanced depending on the length of the spacer. Such an understanding of the properties upon membrane formation from this new class of gemini lipids will be useful for further development of related gene delivery systems.

Introduction

Liposomes resemble closely biological lipid membranes and have been used as ideal candidates for many biological applications.[1] For instance, the use of cationic liposomes for the transfer of nucleic acids into primary or cultured cells in vitro is now a well-established technique.[2,3] There are also rapidly increasing uses of cationic liposomes for the gene delivery in vivo of both marker and potentially therapeutic genes.[3−7] Clearly, detailed understanding of the lipid aggregation is important for the design of better gene transfer agents.

While researchers have delved deeper into the properties of the "monomeric" natural lipids, there are only a few reports in the literature that deals with "multimeric" or "dimeric" (gemini) lipids.[8−10] Gemini lipids belong to a class of amphiphilic molecules typically containing two headgroups and four aliphatic chains linked by a rigid or a flexible spacer. We have already reported the synthesis and membrane-forming properties of pseudoglyceryl gemini lipids.[11,12] It was shown that the introduction of the polymethylene spacers between the cationic ammonium headgroups brings about dramatic effects on the aggregation behavior, membrane organization, and lipid packing of gemini lipids. Recently, we presented the thermotropic and hydration behavior of pseudoglyceryl gemini lipids possessing polymethylene or oxyethylene spacers.[13,14]

To further utilize the unusual behavior of such gemini lipids, we thought of generating an alternative type of gemini lipids where the hydrocarbon chains are anchored via aromatic backbone, which also possess a charged headgroup residue (Figure 1).[15] Although the transfection and aggregation properties of a few cationic lipids based on aromatic backbone are known in literature,[16−19] and many aromatic backbone based compounds have also been shown to have liquid-crystalline properties,[20−27] there is no report that examines the membrane-forming behavior of gemini lipids possessing aromatic backbone. Notably, the presence of sp^2 hybridized planar aromatic hydrocarbon rings at the hydrocarbon chain−polar headgroup linkage region poses interesting situations pertaining to their interlipidic interactions in the membranes as opposed to those based on pseudoglyceryl backbones, which associate with each other and the interfacial water *via* hydrogen bonding and dipolar interactions. Clearly, understanding the surface hydration of such membranes and their packing in aggregates are of importance for their utilization as gene delivery agents.

For the past few years, we have been examining the role of various molecular level modifications on the membrane-forming and transfection properties of different lipids.[28−35] Most of these lipids are based on natural glycerol based or cholesterol based architectures, and herein we present an alternative type of lipids where an aromatic backbone has been anchored between the

* To whom correspondence should be addressed. Phone: (91)-80-2293-2664. Fax: (91)-80-2360-0529. E-mail: sb@orgchem.iisc.ernet.in.
† Indian Institute of Science.
‡ Chemical Biology Unit of JNCASR.

10.1021/jp0750203 CCC: $37.00
Published on Web 11/09/2007

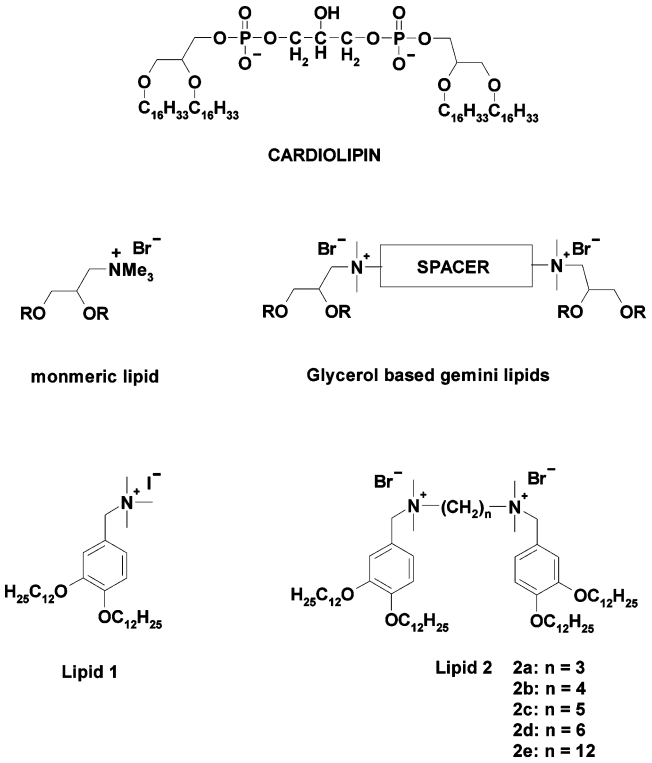

Figure 1. Molecular structures of natural gemini lipid cardiolipin and synthetic gemini lipid based on glycerol backbone and aromatic backbone (**2a**−**2e**) and the corresponding monomeric lipid **1**.

hydrocarbon chains and cationic headgroups (Figure 1).[15] Membrane-forming properties of both the monomeric and the gemini lipids possessing aromatic backbone have been investigated in detail using transmission electron microscopy (TEM), dynamic light scattering (DLS), X-ray diffraction, high-sensitivity differential scanning calorimetry (DSC), Paldan fluorescence studies, and UV−vis absorption spectroscopy. Thermal properties of the gemini lipid aggregates depend strongly on the spacer chain length. In contrast to the aggregates of monomeric lipid, the surfaces of the gemini lipid suspensions in their solid-gel states were considerably "dry". However, above their phase-transition temperatures, these membranous interfaces become highly "wet". The surface hydration also depends on the spacer chain length in such gemini lipids. Closer examination by UV−vis studies suggests the existence of H-type of aggregates in gemini lipid aggregates.

Results and Discussion

Synthesis. In this study, we have synthesized five new gemini lipids (**2a**−**2e**) bearing identical *n*-$C_{12}H_{25}$ chains and have compared their membrane-forming properties with that of their monomer counterpart **1**. These lipids possess an aromatic backbone between the hydrocarbon chains and the cationic headgroup. In gemini lipids, two cationic ammonium headgroups are joined through flexible polymethylene spacers, which differ in length. For the synthesis of gemini lipids, the precursor 1-(3,4-didodecyloxyphenylmethyl)dimethyl amine **3** (Scheme 1) was first synthesized using the same synthetic schemes described previously using *n*-dodecyl bromide instead of *n*-hexadecyl bromide.[15]

The gemini cationic lipids possessing polymethylene spacers **2a**−**2e** were synthesized by heating the precursor 1-(3,4-didodecyloxyphenylmethyl)dimethyl amine **3** with the appropriate α,ω-dibromoalkanes to 80 °C in a mixture of MeOH−EtOAc (1:1) for 48−96 h in screw-top pressure tube (Scheme 1). All the gemini lipids were purified by repeated crystallizations from mixtures of MeOH and EtOAc and were obtained as off-white solids, and the isolated yields of the lipids ranged from 40 to 50%. Monomeric lipid **1** was synthesized by quaternizing the 1-(3,4-didodecyloxyphenylmethyl)dimethyl amine **3** with MeI in dry EtOH.[15]

SCHEME 1[a]

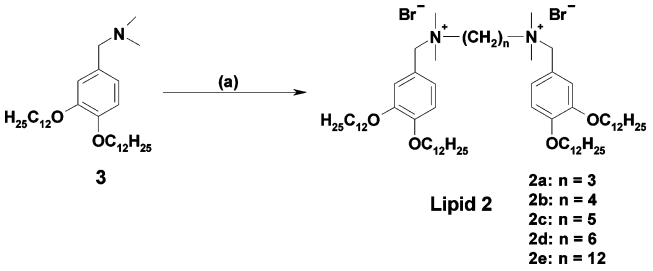

[a] Reagents and conditions: (a) α,ω-dibromo alkanes, MeOH−EtOAc, 48−96 h.

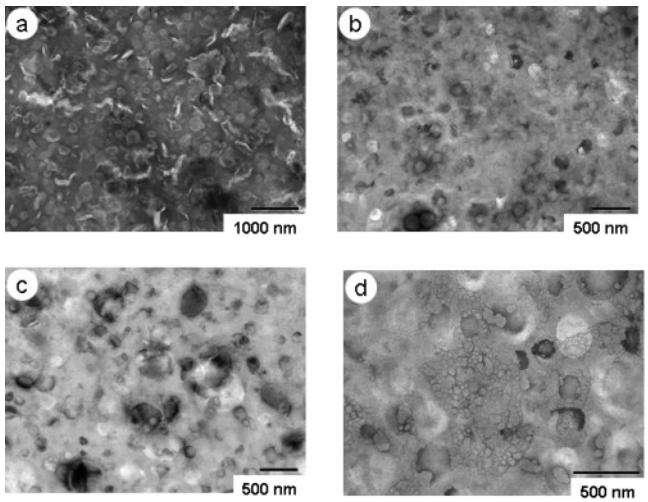

Figure 2. Representative transmission electron micrographs (negatively stained) of aqueous suspensions of cationic lipids (a) **1**, (b) **2b**, (c) **2c**, and (d) **2e**.

Aggregate Characterization. Upon hydration, all the gemini lipids were found to get dispersed in water easily above their phase-transition temperatures (>70 °C). The suspensions formed from each gemini lipid were generally translucent while that of the monomer was found to be optically clearer. All the lipid molecules mentioned herein formed stable suspensions in water and formed unilamellar aggregates upon bath sonication for 15 min above 70 °C. Representative TEM images obtained for these lipid suspensions are shown in Figure 2. Interestingly, the aggregates of all gemini lipids (**2a**−**2e**) possessed smaller average size than that of their monomeric counterpart **1**. Monomeric lipid aggregates afforded vesicles of sizes that varied from 150 to 250 nm, whereas the aggregates from all gemini lipids ranged in sizes that were within 50−200 nm (Table 1). Among the gemini lipids, the lipid **2e** furnished aggregates of smaller size than the other gemini lipids.

The average hydrodynamic diameters of the individual lipid aggregates as revealed by dynamic light scattering (DLS) studies are presented in Table 1. All the lipids showed unimodal distributions of the average populations. DLS results showed that the gemini lipids **2a**, **2d**, and **2e** bearing $-(CH_2)_3-$, $-(CH_2)_6-$, and $-(CH_2)_{12}-$ spacers possessed higher hydro-

TABLE 1: Average Diameter and Aggregate Layer Width of Lipid Suspensions of Gemini Lipids 2a−2e and Monomeric Lipid 1

lipid	size (nm)[a]	size (nm)[b]	width (Å)[c]
1	120	150−250	47.4
2a	220	60−80	46.4
2b	155	100−200	45.5
2c	140	100−200	45.8
2d	260	80−150	50.4
2e	250	40−75	52.1

[a] Hydrodynamic diameters obtained from DLS measurements. [b] As observed from TEM. [c] Unit bilayer thickness from XRD experiments.

dynamic diameters, whereas aggregates from other gemini lipids were of smaller size. Thus, there is no regular trend in the hydrodynamic sizes as a function of spacer chain lengths among gemini lipids. However, this unusual feature of these gemini lipids possessing $-(CH_2)_3-$, $-(CH_2)_6-$, or $-(CH_2)_{12}-$ spacers was also evident from the results of DSC studies, where comparatively high T_m values were observed with these lipid aggregates. It is not apparent why the hydrodynamic sizes or thermal melting temperatures are larger for **2a**, **2d**, and **2e** compared to other geminis. Interestingly, the lipid aggregate sizes obtained from TEM were generally smaller than that obtained from DLS for geminis. In contrast, the sizes obtained from TEM were larger than that obtained by DLS for the monomeric lipid **1**. For TEM studies, samples are usually prepared after wicking of the excess solvent followed by air drying. Therefore, during this process, there can be shrinkage of the aggregates because of the removal of the excess solvent which leads to smaller size aggregates. Alternatively, the fusion of the aggregates is also possible depending upon the lipid structure and aggregate morphology. In the case of lipids **2a**, **2d**, and **2e**, the smaller size of the lipid aggregates observed under TEM could be due to such a drying effect. In the case of monomeric lipid **1**, however, larger lipid aggregates were observed which could be because of the fusion of the lipid aggregates. The difference in the behavior (shrinkage vs fusion) under TEM conditions could be because of the intrinsic differences in the lipid character (monomeric vs gemini). On the other hand, in the case of lipid **2b** and **2c** aggregates, the hydrodynamic diameters and sizes from TEM studies were in reasonably good agreement with each other.

X-ray diffraction experiments with self-supporting cast films of the aqueous suspensions of **2a**−**2e** showed the existence of a series of higher order reflections characteristic of lamellar phases in their diffraction pattern (not shown). The unit lamellar widths of individual lipid aggregates are given in Table 1. Incorporation of polymethylene $-(CH_2)_n-$ spacers between cationic ammonium headgroups did not alter the bilayer thickness of the gemini lipid aggregates significantly except for the lipid **2e** where ~5 Å increase in bilayer width was observed.

In general, the sizes of aggregates formed by all gemini lipids (**2a**−**2e**) were found to be smaller than monomeric counterpart **1**. The hydrodynamic diameters of aggregates formed by all the gemini lipids showed unimodal distributions.

Thermal Behavior of Membranes. To understand the effect of the covalent incorporation of the polymethylene spacer on the phase-transition temperature (solid-gel-like to fluid liquid-crystalline phase) of these lipid aggregates, differential scanning calorimetry (DSC) studies have been performed. Well-behaved gel to liquid-crystalline phase transitions were obtained from all the lipids, and all the lipid suspensions showed partially reversible transitions in DSC (Figures 3 and 4). The thermotropic properties as obtained from DSC of aggregates of all the gemini lipids and their monomeric counterpart are summarized in Table 2. A temperature lag was observed in thermograms of the cooling scans (fluid-to-solid phase transition) of all the suspensions of gemini lipids (**2a**−**2e**) as well as that of monomeric lipid **1** (Figures 3 and 4). Such a hysteresis was found to be very much dependent upon the length of the spacer chain in gemini lipids. Gemini lipid **2e** showed the maximum hysteresis of ~8 °C, whereas other gemini lipids showed hysteresis of ~3 °C. Such temperature lags are characteristics of a first-order lipid phase transition.[36]

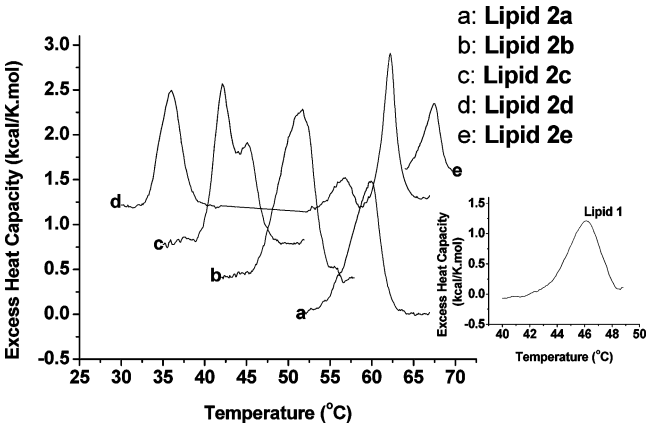

Figure 3. Thermotropic phase transitions as evidenced by the DSC on heating scans. Thermograms of lipid **2b**−**2e** aggregates have been successively raised from the baseline by 0.4 kcal/(K.mol) steps for clarity. Inset shows the thermotropic phase transition of monomeric lipid **1** aggregates on heating scan.

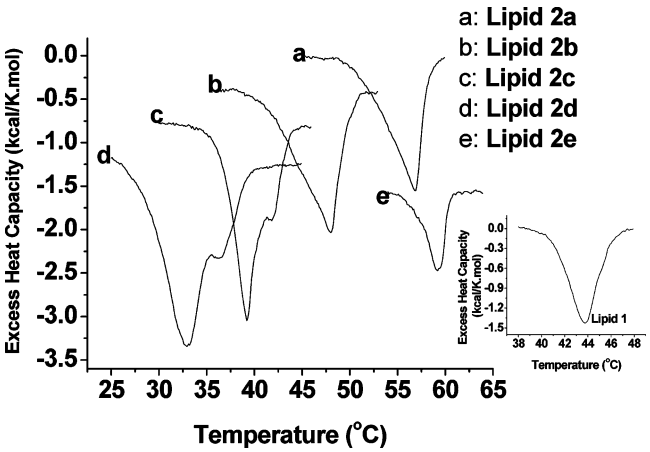

Figure 4. Thermotropic phase transitions as evidenced by the DSC on cooling scans. Thermograms of lipid **2b**−**2e** aggregates have been successively lowered from the baseline by 0.4 kcal/(K.mol) steps for clarity. Inset shows the thermotropic phase transition of monomeric lipid **1** aggregates on cooling scan.

TABLE 2: Thermotropic Parameters as Obtained from DSC Studies with Various Lipid Suspensions

	T_m (°C)[a]		ΔH_c (kcal/mol)[b]	ΔS (kcal/K.mol)[c]	CU[d]
lipid	upscan	downscan	upscan	upscan	upscan
1	46.1	43.8	4.4	0.014	109
2a	59.9	56.9	6.5	0.019	56
2b	51.7	48.0	9.5	0.029	30
2c	42.1	39.2	7.5	0.024	32
2d	36.0, 62.2	32.9	4.0, 4.6	0.013, 0.014	111, 215
2e	67.4	59.2	1.8	0.005	360

[a] Maximum deviation was ±0.1 °C. [b] Values varied within ±0.2 kcal/K.mol. [c] Values varied within ±0.002 kcal/K.mol. [d] Size of cooperativity unit.

The gemini lipids show considerable differences in their phase-transition temperatures (T_m) in spite of having identical hydrocarbon chain length (n-$C_{12}H_{25}$) and the same electrostatic character as shown in Table 2. Incorporation of the propanediyl spacer [$-(CH_2)_3-$] between the cationic ammonium headgroups of monomeric lipid dramatically increased the T_m values to ~60 °C as compared to the monomer, which gave a T_m value of only ~46 °C. We had observed similar enhancement in the T_m for pseudoglyceryl gemini lipids possessing propanediyl [$-(CH_2)_3-$] spacer segment with n-$C_{14}H_{29}$ or n-$C_{16}H_{33}$ hydrocarbon chains.[14] This increase in T_m value is presumably because of the close proximity of the lipid chains in the aggregates of gemini lipid **2a**. In aqueous suspension of the gemini lipids bearing polymethylene spacer, the two covalently charged $-N^+Me_2$ headgroups tend to maintain a critical distance between them to minimize the columbic repulsions. However, since this situation would create rather an unfavorable contact of the hydrophobic $-(CH_2)_{n-}$ spacer chain with the bulk water, a separation based on compromise of these two opposing tendencies should result.[37] In the case of lipid **2a**, because of the presence of a short propanediyl spacer between the $-N^+Me_2$ headgroups, the hydrophobic chains come close leading to manifest an increase in the T_m value. With further increase in the spacer length from propanediyl [$-(CH_2)_3-$] to pentanediyl [$-(CH_2)_5-$], the T_m value decreased to ~42 °C. The lipid **2c** also showed a transition at a higher temperature (~45 °C) than the main transition (gel to liquid-crystalline transition). Similarly, during the cooling scan of gemini lipid **2c**, a pretransition at ~42 °C, followed by a transition at 39 °C, was observed. This shows that with increase in the spacer length, the distance between the lipid chains in a gemini lipid increases, presumably leading to less efficient hydrocarbon chain packing which further leads to the decrease in T_m values. These observations are similar with the thermotropic behavior of the pseudoglyceryl gemini lipids.[14] Gemini lipid **2d**, with hexanediyl [$-(CH_2)_6-$] spacer, showed a more complex DSC thermogram where two phase-transition temperatures of comparable intensity were observed at 36 °C and 62.2 °C with a pretransition at ~57 °C. During cooling scans, only one transition was observed at ~33 °C. The complex behavior of the gemini lipid **2d** during the heating scan of DSC became clear from the temperature-dependent UV−vis absorption of the lipid aggregate studies as discussed later. Aggregates of gemini lipid **2e** with dodeanediyl [$-(CH_2)_{12}-$] spacer showed the highest phase-transition temperature of ~67 °C in this series.

A temperature lag of ~8 °C (maximum in the series) was observed during the cooling scan of the aggregates of lipid **2e**. This observation of maximum temperature lag in the case of lipids possessing [$-(CH_2)_{12}-$] spacer was also observed with pseudoglyceryl gemini lipids bearing the spacer of the same length.[14] This suggests that a highly stabilized "liquid-crystalline" fluid phase might exist in the lipid aggregates of **2e**. It is possible that, upon melting, the lipid aggregates of **2e** become significantly more hydrated than in its solid-gel state. Cooling of the melted lipid aggregates at their full hydration may not immediately favor the release of the water molecules from these aggregates prior to its transition to gel state. The evidence of high hydration state of gemini lipid **2e** aggregates has also been shown by Paldan fluorescence studies as described later.

In general, the enthalpy of transition of the heating scan was higher for all the gemini lipids in comparison with that of their corresponding monomer except for lipid **2e**. Interestingly, all the lipids showed higher enthalpy contribution during their cooling scan (liquid-crystalline to solid-gel phase transition) than during their heating scan except lipid **2b**. Similarly, entropy of transition of the heating scan was higher for all the gemini lipids in comparison with their corresponding monomer except for lipid **2e**. All the lipid aggregates showed higher entropy contribution during their cooling scan (fluid-to-solid phase transition) than during their heating scan. The gemini lipid aggregates were found to be less cooperative than that of the monomeric lipid **1** both from solid-gel to liquid-crystalline transition and from fluid to solid state as well except for that of lipid **2e**, which showed the maximum cooperativity. Overall, among the gemini lipids, the lipid **2e** showed unusual features of highest T_m, lower calorimetric enthalpy and entropic contribution, highest hysteresis, and high cooperativity during phase transition.

TABLE 3: Fluorescence Characteristics of Paldan in Lipid Aggregates of 1 and 2a−2e

	λ_{em} (nm)[a]		GP		FWHM[b]	T_m
lipid	24 °C	70 °C	24 °C	70 °C	(nm)	(°C)
1	471.6	472.0	−0.109	−0.160	88.6	[c]
2a	438.8	489.8	0.332	−0.398	78.1	59
2b	441.4	470.6	0.242	−0.173	95.4	52
2c	431.2	459.4	0.437	0.102	81.3	42
2d	423.6	483.8	0.549	−0.299	57.8	36
2e	464.6	484.8	−0.039	−0.291	105.6	[c]

[a] Emission monitored at 440 nm. [b] Full width at half-maxima (nm) at 24 °C. [c] Could not be measured because of absence of any detectable transition.

Polarity of the Membrane Interfaces. The hydration of the interfaces of these lipid aggregates was estimated by measuring the steady-state fluorescence emission using a polarity-sensitive fluorophore, Paldan. Prodan and Laurdan, which are propyl and lauryl derivatives of the 6-dimethylamino naphthalene, are well-studied fluorophores used to determine the hydration of the lipid vesicles. Paldan is the palmitoyl derivative of 6-dimethylamino naphthalene, and here the hydrocarbon chains of the probe closely match the length of the hydrophobic parts of the lipids studied. Therefore, Paldan should get appropriately immersed in the vesicles and should report the microenvironment at the membrane surface more correctly than other probes like pyrene, ANS, tryptophan, and so forth. Paldan like Prodan or Laurdan is a fluorescent probe that exhibits strong shifts in the absorption and emission spectra upon variation of polarity of the environment. It emits an intense, broad fluorescence band that is strongly red-shifted with increasing polarity−polarizability and the hydrogen donor ability of the media. Therefore, compared to other probes, Paldan would provide more realistic information about the hydration on the membrane surface. The fluorescence characteristics of Paldan (not shown) were similar to that of its lauroyl analogue, Laurdan.[40] The important parameters obtained from the experiments using Paldan fluorescence with lipid aggregates are summarized Table 3.

The emission λ_{max} of Paldan in the gel state of aggregates of monomeric lipid **1** was found to be ~472 nm, whereas in the case of all the gemini lipid aggregates (**2a**−**2d**) except that of lipid **2e**, the λ_{max} of Paldan appeared in the range of 420−440 nm. The pronounced blue-shift (32−52 nm) in the emission λ_{max} of Paldan fluorescence in the case of all gemini lipids (**2a**−**2d**) except for lipid **2e** indicates that the surfaces of all gemini lipid aggregates except that of **2e** are less hydrated in their gel states as compared to that of the monomeric lipid **1**. Red-shift in the emission λ_{max} upon melting of a lipid aggregate is a consequence of increased water penetration into the lipid interior during melting.[41] In the fluid state of the aggregates of monomeric lipid **1**, above phase-transition temperature, no shift in the λ_{max} was

observed, indicating that the monomeric lipid **1** was already in its maximal hydrated state in the solid-gel phase. This indirectly suggests that strong supramolecular interactions still hold together the lipid molecules in the fluid state of the monomeric lipid **1** aggregates in such a way that significant penetration of the water molecules is not allowed. This will become clearer as we discuss UV−vis studies later. In contrast, the emission maxima due to Paldan doped in the aggregates of gemini lipids (**2a**−**2e**) were dramatically shifted to higher wavelengths in the fluid melted states. For instance, at 24 °C in the solid-gel phase, the emission λ_{max} of Paldan in lipid **2a** aggregates was 438 nm, which shifted to 489 nm in the melted state (Table 3). Similarly, in the case of other gemini lipids, pronounced red-shift was observed. Maximum red-shift was observed for the aggregates of lipid **2d** (60 nm) and minimum was observed for that of lipid **2e** (20 nm) aggregates. This means that the aggregates of lipid **2d** were least hydrated and that of **2e** was most hydrated in their solid-gel states. As mentioned earlier, such a long wavelength emission λ_{max} is a characteristic of a highly hydrated state.[41] This clearly shows that all gemini lipid aggregates were in highly hydrated states in their fluid liquid-crystalline phase unlike the aggregates of their monomeric counterpart **1**.

The excitation spectra (not shown) of Paldan in all lipid aggregates were similar to that of monomeric lipid analogue both in their gel and liquid-crystalline phases. This further confirms the fact that the emission characteristics of Paldan in these novel gemini lipid aggregates were purely due to the excess solvent (water) mediated stabilization of the excited state and were not due to any inherent differences in its ground states in these lipid aggregates.[42]

Generalized polarization (GP) is taken as a measure of the extent of hydration in the case of 6-dimethylamino naphthalene based fluorescent probes such as Prodan and Laurdan.[42,43] The GP of such membrane-soluble probe is strongly affected by the phase state (gel vs liquid-crystalline) of the membrane. Variation of GP as a function of temperature often shows an abrupt change at the lipid phase transition. It is well-established that more positive values of GP correlate well with low surface hydration of membranes and that more negative values of GP correlate to high surface hydration of the lipid aggregates. Lipid aggregates, in their gel states, exhibit generally a high value of GP which decreases upon melting to the liquid-crystalline state because of the increased water penetration into the bilayer interior during melting, which also leads to the manifestation of more red-shifted emission of the fluorophore.

The GP values obtained with the various lipid aggregates are given in Table 3. It was observed that the water penetration as sensed by Paldan was lower for all gemini lipid (**2a**−**2e**) aggregates as compared to that of monomeric lipid **1** in the gel state. In the melted state, all gemini lipids except lipid **2c** possessed lower GP value as compared to that of the monomeric lipid **1**, which further demonstrated the more hydrated behavior of gemini lipids. Moreover, the emission spectrum of Paldan in all gemini lipid aggregates except that of lipid **2a** was comparatively broader than that in monomeric lipid. This is indicative of fluorescence emissions from multiple excited states, arising probably because of differential solvent relaxation.

The generalized polarization (GP) versus temperature profiles in Figure 5 show systemic breaks related to the main thermotropic phase-transition processes for individual lipid assemblies except for lipid aggregates **1** and **2e**. Lipid **1** was found to be already quite hydrated in its gel states. Because of this and because of an increase in temperature, there is no abrupt rise in the hydration of these lipid aggregates, which is evidenced from

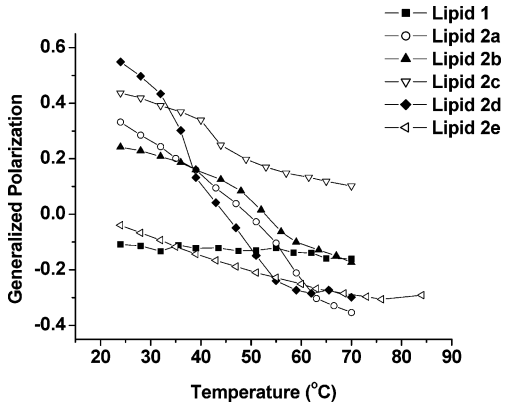

Figure 5. Changes in the generalized polarization of Paldan doped in gemini aggregates of the lipids **1** and **2a**−**2e** as a function of temperature.

their nearly monotonous decrease of GP values with increasing temperature. Similarly, lipid **2e** aggregates were found to be also highly hydrated already in their gel states and, with increase in temperature, there was little decrease in GP values because of already high hydrated nature of these aggregates. This explains why we observed monotonous profiles of GP against temperature (without a break) for the lipid **1** and **2e** aggregates. The phase-transition temperature for all the gemini lipid membranes decreased with the increase in the spacer length presumably because the increase in spacer length leads to greater separation between the cationic ammonium headgroups. The transition temperatures obtained from the Paldan studies correlated reasonably well to that obtained from the DSC studies. Comparison of the hydration behavior of the present set of gemini lipid aggregates with that of pseudoglyceryl gemini lipids possessing *n*-$C_{16}H_{33}$ hydrocarbon chains shows that the lipids with dodeanediyl [$-(CH_2)_{12}-$] spacer are always more hydrated as compared to other gemini lipids.[14] Aromatic monomeric lipid **1** is more hydrated as compared to its gemini lipids in contrast to pseudoglyceryl lipids, where gemini lipids are more hydrated as compared to monomeric lipid.[14] These differences could be attributed to the differences in the microenvironment of the membrane organization of the aromatic lipid aggregates as compared to that of pseudoglyceryl lipid aggregates.

UV−Vis Spectra of Aggregates. After investigating the thermal properties by differential scanning calorimetry and temperature-dependent changes in hydration of the membranous interfaces, we sought to understand how the lipid units possessing aromatic backbones interact in their aggregates. To identify the involvement of the aromatic moiety of the lipids, we performed the UV−vis absorption spectra of the lipid solutions in chloroform and their aggregates in water. All the lipids in chloroform gave characteristic absorption spectra, having two peaks at ∼250 and ∼285 nm. In aggregate state of all the lipids in aqueous media, a new blue-shifted peak was observed at ∼200 nm (Figure 6).

In the aggregated states, these lipid molecules could arrange themselves in various ways because of the presence of aromatic planar surface, for example, J-type or H-type aggregates.[44,45] The J-aggregate is a one-dimensional molecular arrangement in which the transition moments of individual monomers are aligned parallel to the line joining their centers (end-to-end arrangement). The H-aggregate is an alternative one-dimensional array of molecules in which the transition moments of individual monomers are aligned parallel to each other but perpendicular to the line joining their centers (face-to-face arrangement). The most characteristic feature of J-aggregate is that they exhibit a

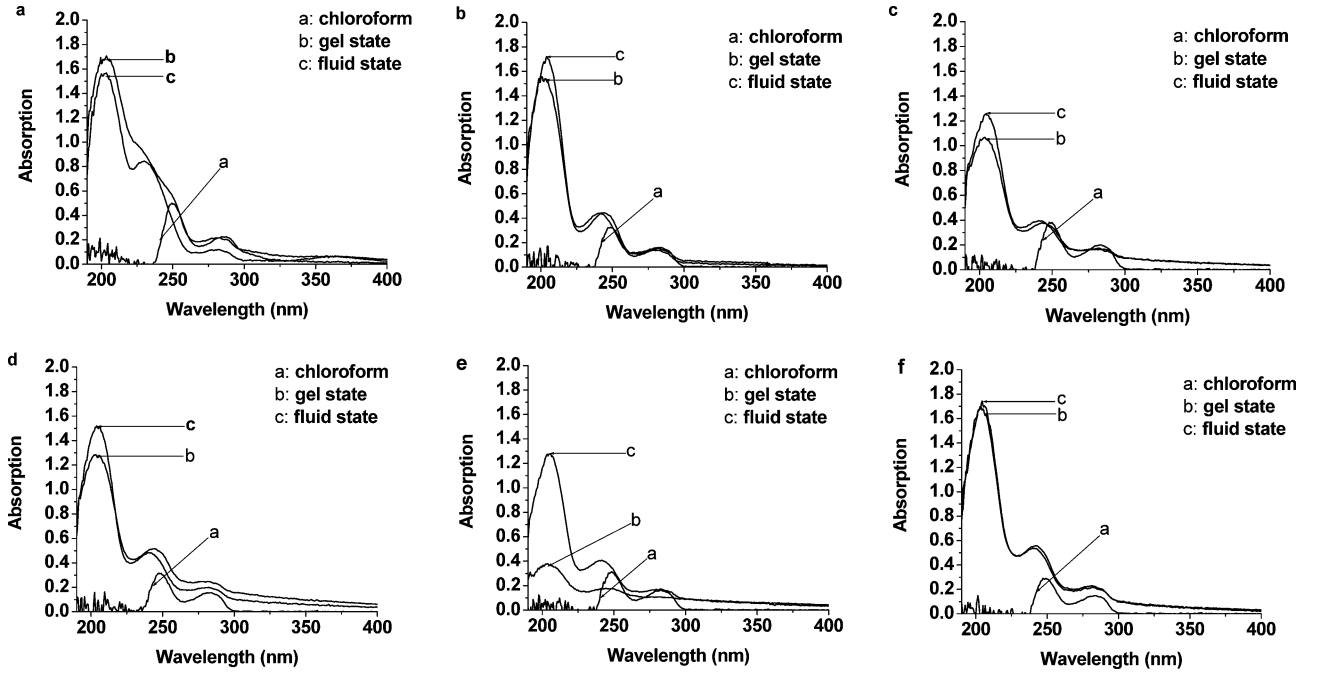

Figure 6. UV−vis absorption spectra of the gemini cationic lipids as solution in chloroform and as aggregated in water (both in gel and fluid phase). (a) Lipid **1**, (b) lipid **2a**, (c) lipid **2b**, (d) lipid **2c**, (e) lipid **2d**, and (f) lipid **2e**.

narrow peak (J-band) red-shifted in the absorption spectrum with respect to its monomer absorption. The absorption spectrum of the H-aggregate consists of a blue-shifted band (generally not as narrow as the J-band) with respect to the monomer absorption. Therefore, in the present set of lipid aggregates, H-type aggregates between the lipid molecules were most likely formed, as we observed a blue-shifted band (H-band) at ∼200 nm in the case of all the lipid aggregates (Figure 6) as compared to the absorption spectrum of chloroform solution of respective lipid.

To see the effect of the temperature on the lipid aggregates, we then examined the absorption spectra of all the lipid aggregates both in the gel state (24 °C) and in the fluid state (80 °C). In the fluid state, we observed a little decrease in the intensity of the H-type band (∼200 nm) in the case of monomeric lipid **1**. The decrease in the intensity of the H-band in the case of monomeric lipid **1** most likely indicates that the stacking between the aromatic faces is breaking, although there is no complete breakage of these H-aggregates, which occurs only at very high temperature. In the case of all gemini lipids (**2a**−**2d)** except **2e**, interestingly, there is an increase in the intensity of the H-band. An increase in the intensity of the H-band in the case of all the gemini lipids (**2a**−**2d**) indicates that there is an increase in H-aggregate formation. This further suggests that the polymethylene spacer, which loops inward toward hydrophobic interior in the solid-gel phase, comes out. This drives the aromatic surfaces of each lipid units to come close, leading to an increase in the H-band intensity. This increase in H-band intensity is very much dependent on the length of the spacer, being maximum for gemini lipid possessing hexamethylene $-[(CH_2)_6]-$ spacer. Therefore, in the fluid phase, the spacer chain $-(CH_2)_6-$ loops outward toward bulk water, which brings the aromatic surfaces of gemini lipids closer. This increase in stacking further increases the intensity of the H-band. In fluid phase, although there would be unfavorable interactions of the spacer with water, these interactions would be compensated and probably overtaken by the $\pi-\pi$ stacking interactions present in H-aggregates. In the case of gemini lipids (**2a**−**2c**), lengths of the spacer are not sufficient to allow the aromatic

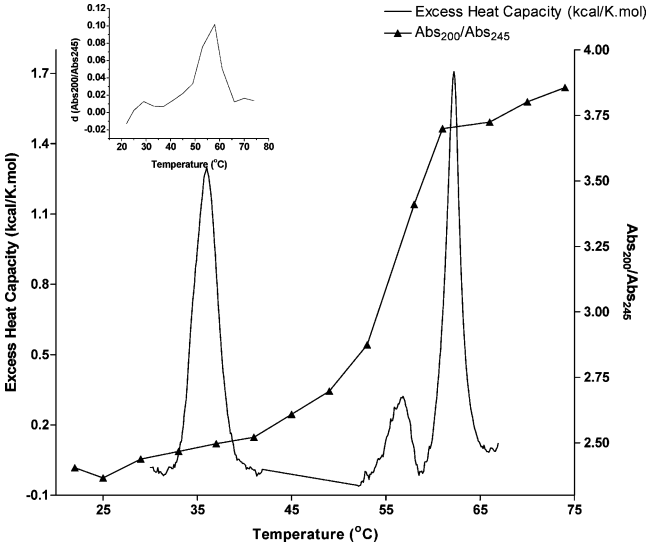

Figure 7. Overlay of the heating DSC thermogram of the gemini lipid **2d** aggregates and the effect of the temperature on the Abs_{200}/Abs_{245}. Inset shows the $d(Abs_{200}/Abs_{245})$ vs temperature.

surfaces to come very close, whereas in case of gemini lipid **2e**, the length of the flexible spacer is too long such that the $\pi-\pi$ interactions cannot overtake the unfavorable interactions of the long polymethylene spacer $-(CH_2)_{12}-$ with water molecules. Therefore, there is no increase in the intensity of the H-band in the fluid state in the case of lipid **2e** aggregates. There is minimal effect on other absorption bands upon aggregation formation except for that of the monomeric lipid **1**, where a blue-shift in the ∼245 nm band was observed.

The change in Abs_{200}/Abs_{245} in the case of lipid **2d** aggregates as a function of temperature is presented in Figure 7, overlaying the heating scan observed from the DSC. The heating scans of the gemini lipid **2d** aggregates show complex thermogram. One question comes in mind: what could be the reason behind such complex phenomenon? The Abs_{200}/Abs_{245} versus T profile indicates two clear breaks at 30 °C and 58 °C. These two peaks quite adequately correspond to the T_m values obtained from the

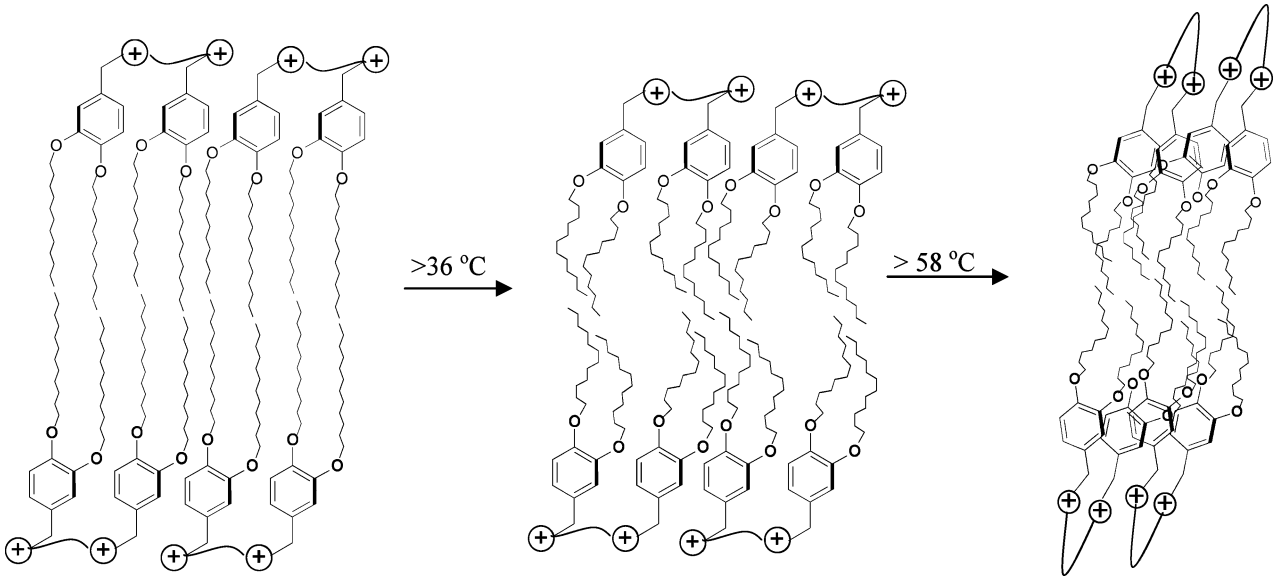

Figure 8. Schematic representation of the effect of the temperature on gemini lipid **2d** aggregates.

DSC studies, although these values are slightly lower than that obtained from DSC studies. This could be due to differences in the sensitivities in two different physical measurements. We hypothesized the membrane organization of the gemini lipid **2d** aggregates as shown in Figure 8. In the gel phase, <36 °C, the hydrocarbon chains are in fully staggered form and are packed tightly. The aromatic moieties of gemini lipids had $\pi-\pi$ interactions as evidenced from the UV spectra of lipid aggregates (Figure 6e). With increase in temperature (>36 °C in DSC), first the hydrocarbon chains get distorted as evidenced by very little change in the Abs_{200}/Abs_{245} value. In the fluid phase of the membranes (>60 °C), there was dramatic increase in Abs_{200}/Abs_{245} value, which is due to stronger $\pi-\pi$ interactions. Therefore, at higher temperature (60 °C in DSC), the $-(CH_2)_6-$ spacer comes out of the hydrophobic interior of the membrane. This creates unfavorable interactions of the $-(CH_2)_6-$ spacer with water molecules. However, these unfavorable interactions are compensated by the $\pi-\pi$ interactions at higher temperature which leads to an increase in Abs_{200}/Abs_{245} value.

Conclusions. Here, we report the unusual aggregation properties of a new kind of gemini lipids based on aromatic backbone. The insertion of the aromatic unit between the hydrocarbon chains and the polar headgroup radically influences the aggregation behavior of these gemini lipids. The length of the spacer dramatically affects the membrane-forming properties and the surface hydration of the membranes formed from these gemini lipids. The membrane-forming properties of these gemini lipids clearly differ from that of gemini lipids based on pseudoglyceryl backbone.[14] Incorporation of the aromatic ring between the headgroup and the hydrocarbon chains favors the $\pi-\pi$ stacking interactions between the lipid molecules in their aggregates, and these aggregations strongly depend upon the length of the spacer between the headgroups. This aggregation behavior of these aromatic backbone based gemini lipids further affects the hydration properties of these aggregates, which are also found to be dependent upon the length of the spacer segment. These new findings highlight the need for the new design of lipid molecules to further increase our understanding about membranous aggregates and their utilization in gene transer.[46]

Experimental Section

Materials and Methods. All reagents, solvents, and chemicals used in this study were of the highest purity available. The solvents were dried prior to use. Column chromatography was performed using 60−120 mesh silica gel. NMR spectra were recorded using Jeol JNM λ-300 (300 MHz for ^{1}H) spectrometer. The chemical shifts (δ) are reported in ppm downfield from the internal standard, TMS, for ^{1}H NMR. Mass spectra were recorded on a Kratos PCKompact SEQ V1.2.2 MALDI-TOF spectrometer or on a MicroMass ESI-TOF spectrometer or on a Shimadzu table-top GC-MS or ESI-MS (HP1100LC-MSD). Infrared (IR) spectra were recorded on a Jasco FT-IR 410 spectrometer using KBr pellets or neat. Cationic lipids were synthesized as described below and were characterized fully by their ^{1}H NMR, mass spectra, and elemental analysis.

Synthesis. *General Method for Synthesis of Gemini Lipids (**2a**−**2e**).* A solution of 1-(3,4-didodecyloxyphenylmethyl)-dimethyl amine (**3**) 120 mg (0.24 mmol) and appropriate α,ω-dibromo alkane (0.080 mmol) in dry MeOH/EtOAc mixture was refluxed over a period of 48−96 h. It was cooled, and the solvent was evaporated to give a crude solid. It was repeatedly washed with dry EtOAc to remove unreacted starting material and finally was subjected to repeated crystallization from a mixture of EtOAc and MeOH (9:1), which gives a white solid. Yield: 40−50% (exact yield depends on the corresponding alkane dibromide). ^{1}H NMR, mass spectral data, and elemental analysis of all the lipids have been presented in the Supporting Information.

Vesicle Preparation. Thin films from individual lipids were prepared in glass vials by dissolving weighed amounts of individual lipids in chloroform and by evaporating the organic solvent under a stream of dry nitrogen. The last traces of organic solvent were removed by keeping these films under high vacuum for 5−6 h. The required amount of water (Milli Q) was added to each individual film and was kept for hydration at 4 °C for 1 day. Then, the suspension was thawed to 70 °C for 10 min, was vortexed for 5 min, and then was frozen to 0 °C for 10 min. Each sample was subjected to five to six freeze−thaw cycles to ensure optimal hydration. Unilamellar aggregates were

prepared by further sonication of these aggregates in a bath sonication at 80 °C for 15 min as indicated by electron microscopy.

Transmission Electron Microscopy. Unilamellar suspension of each cationic lipid (1 mM) was examined under transmission electron microscopy by negative staining using 1% uranyl acetate. A 15 μL sample of the suspension was loaded onto Formvar-coated, 400 mesh copper grids and was allowed to remain for 1 min. Excess fluid was wicked off the grids by touching their edges to filter paper, and 15 μL of 1% uranyl acetate was applied on the same grid after which the excess stain was similarly wicked off. The grid was air-dried for 30 min, and the specimens were observed under TEM (JEOL 200-CX) operating at an acceleration voltage of 120 keV. Micrographs were recorded at a magnification of 4000−20 000×.

Dynamic Light Scattering. Unilamellar vesicles (1 mM) prepared in pure water (as mentioned under vesicle preparation) were diluted to 0.33 mM and were used for dynamic light scattering measurements. Experiments were performed using a Malvern Zetasizer 3000 instrument, which employed an incident laser beam of 633 nm. An interfaced autocorrelator was used to generate the full autocorrelation of the scattered intensity. The time-correlated function was analyzed by the method of cumulants, and calculations yielded specific distribution of particle size populations. The values reported are the averages of two independent experiments, each of them having 10 subruns.

Cast-Film X-ray Diffraction Measurements. The experiment was done following the reported procedures.[47,48] Twenty microliters of lipid suspension of each lipid (3 mM) in water was placed on a precleaned glass plate which, upon air-drying, afforded a thin film of the lipid aggregate on the glass plate. X-ray diffraction of individual cast films was performed using the reflection method with a Rich Seifert-3000 TT X-ray diffractometer. The X-ray beam was generated with a Cu anode and the Cu−K_α beam of wavelength 1.5418 Å was used for the experiments. Scans were performed for 2θ range of 1.3−14° with the scan rate of 1° per min and step size of 0.02.

Differential Scanning Calorimetry. Unilamellar lipid vesicles of 1 mM concentration were prepared in degassed water as mentioned above, and their thermotropic properties were investigated by high-sensitivity differential scanning calorimetry using a CSC-4100 model, multicell differential scanning calorimeter (Calorimetric Science Corporation, Utah). The baseline thermogram was obtained using degassed water (0.5 mL) in all the ampoules including the reference cell to normalize cell-to-cell differences. Samples were taken in the cells such that the differences in weight with the baseline experiment to the sample run were less than 0.001 g in the respective ampoules. The measurements were carried out in the temperature range of 20−90 °C. The scan rate was 20 °C per hour for all the lipids. The thermograms for vesicular suspensions were obtained by subtracting the respective baseline thermogram from the sample thermogram using the software CpCalc provided by the manufacturer. Peak position in the plot of the excess heat capacity versus temperature on heating scan and cooling scan was taken as the solid-like gel-to-fluid phase-transition temperature and the fluid-to-gel phase transition, respectively, for each amphiphilic suspension. The molar heat capacities, calorimetric enthalpies (ΔH), and entropies (ΔS) were also computed using the same software as reported. The size of cooperativity unit (CU) for the phase transition of each lipid was determined using the formula

$$\mathrm{CU} = \frac{\Delta H_{\mathrm{vH}}}{\Delta H_{\mathrm{c}}}$$

where ΔH_{vH} is the vant Hoff enthalpy and ΔH_{c} is the calorimetric enthalpy.[49,50] The vant Hoff enthalpy was calculated from the equation

$$\Delta H_{\mathrm{vH}} = \frac{6.9 T_m^{\,2}}{\Delta T_{1/2}}$$

where $\Delta T_{1/2}$ is the full width at half-maximum of the thermogram and T_{m} is the phase-transition temperature.[50]

Paldan Fluorescence. Paldan, a palmitoyl analogue of Prodan, was synthesized by appropriate modification of literature procedures.[38,39] The spectral properties of Paldan were very similar to that of its other analogues (Prodan and Laurdan). All the fluorescence experiments were carried out on sonicated lipid suspensions using a lipid-to-probe ratio of 1000:1. The width of excitation and emission slit was 5 nm. Generalized polarization (GP)[42,43] of emission (GP) was calculated using the equation

$$\mathrm{GP}_{\mathrm{em}} = \frac{I_{440} - I_{490}}{I_{440} + I_{490}}$$

where I_{440} and I_{490} represent the fluorescent intensities at 440 and 490 nm. For the GP values reported herein, an excitation wavelength of 350 nm was used. For excitation spectra, wavelength was kept at 440 nm unless specified otherwise.

Acknowledgment. This work was supported by Department of Biotechnology, Government of India, New Delhi, India. Avinash Bajaj thanks CSIR for a senior research fellowship.

Supporting Information Available: ^{1}H NMR, mass spectral data, and elemental analysis of all the lipids have been presented in the Supporting Information. This material is available free of charge via the Internet at http://pubs.acs.org.

References and Notes

(1) Bhattacharya, S.; Bajaj, A. *Curr. Opin. Chem. Biol.* **2005**, *9*, 647−655.
(2) Miller, A. *Angew. Chem., Int. Ed.* **1998**, *37*, 1768−1785.
(3) Ewert, K.; Ahmad, A.; Evans, H. M.; Safinya, C. R. *Expert Opin. Biol. Ther.* **2005**, *5*, 33−53.
(4) Wang, J.; Guo, X.; Xu, Y.; Barron, L.; Szoka, F. C., Jr. *J. Med. Chem.* **1998**, *41*, 2207−2215.
(5) Ronsin, G.; Perrin, C.; Guedat, P.; Kremer, A.; Camilleri, P.; Kirby, A. J. *Chem. Commun.* **2001**, 2234−2235.
(6) Hulst, R.; Muizebelt, I.; Oosting, P.; Van der Pol, C.; Wagenaar, A.; Smisterova, J.; Bulten, E.; Driessen, C.; Hoekstra, D.; Engberts, J. B. F. N. *Eur. J. Org. Chem.* **2004**, 835−849.
(7) Karmali, P. P.; Majeti, B. K.; Sreedhar, B.; Chaudhuri, A. *Bioconjugate Chem.* **2006**, *17*, 159−171.
(8) Chien, P.-Y.; Wang, J.; Carbonaro, D.; Lei, S.; Miller, B.; Sheikh, S.; Ali, S. M.; Ahmad, M. U.; Ahmad, I. *Cancer Gene Ther.* **2005**, *12*, 321−328.
(9) Kasireddy, K.; Ali, S. M.; Ahmad, M. U.; Choudhury, S.; Chien, P.-Y.; Sheikh, S.; Ahmad, I. *Bioorg. Chem.* **2005**, *33*, 345−362.
(10) Ilies, M. A.; Seitz, W. A.; Johnson, B. H.; Ezell, E. L.; Miller, A. L.; Thompson, E. B.; Balaban, A. T. *J. Med. Chem.* **2006**, *49*, 3872−3887.
(11) Bhattacharya, S.; De, S.; George, S. K. *Chem. Commun.* **1997**, 2287−2288.
(12) Bhattacharya, S.; De, S. *Chem. Eur. J.* **1999**, *5*, 2335−2347.
(13) Bhattacharya, S.; Bajaj, A. *J. Phys. Chem. B* **2007**, *111*, 2463−2472.
(14) Bhattacharya, S.; Bajaj, A. *Langmuir* **2007**, *23*, 8988−8994.
(15) Paul, B.; Bajaj, A.; Indi, S. S.; Bhattacharya, S. *Tetrahedron Lett.* **2006**, *47*, 8401−8405.
(16) Ilies, M. A.; Seitz, W. A.; Ghiviriga, I.; Johnson, B. H.; Miller, A.; Thompson, E. B.; Balaban, A. T. *J. Med. Chem.* **2004**, *47*, 3744.

(17) Ewert, K.; Ahmad, A.; Evans, H. M.; Schmidt, H.-W.; Safinya, C. R. *J. Med. Chem.* **2002**, *45*, 5023−5029.

(18) Koiwai, K.; Tokuhisa, K.; Karinaga, R.; Kudo, Y.; Kusuki, S.; Takeda, Y.; Sakurai, K. *Bioconjugate Chem.* **2005**, *16*, 1349−1351.

(19) (a) Ewert, K. K.; Evans, H. M.; Zidovska, A.; Bouxsein, N. F.; Ahmad, A.; Safinya, C. R. *J. Am. Chem. Soc.* **2006**, *128*, 3998−4006. (b) Bhattacharya, S.; Subramanian, M.; Hiremath, U. S. *Chem. Phys. Lipids* **1995**, *78*, 177−188.

(20) Ferroukhi, O.; Atik, N.; Guermouche, S.; Guermouche, M. H.; Berdague, P.; Judenstein, P.; Bayle, J. P. *Chromatographia* **2000**, *52*, 564−568.

(21) Nozary, H.; Piguet, C.; Rivera, J.-P.; Tissot, P.; Morgantini, P.-Y.; Weber, J.; Bernardinelli, G.; Buenzli, J.-C. G.; Deschenaux, R.; Donnio, B.; Guillon, D. *Chem. Mater.* **2002**, *14*, 1075−1090.

(22) Boudah, S.; Sebih, S.; Guermouche, M. H.; Rogalski, M.; Bayle, J. P. *Chromatographia* **2003**, *57*, S/307−S/311.

(23) Callau, L.; Reina, J. A.; Mantecon, A. *J. Polym. Sci., Part A: Polym. Chem.* **2003**, *41*, 3384−3399.

(24) Tasaka, T.; Okamoto, H.; Morita, Y.; Kasatani, K.; Takenaka, S. *Mol. Cryst. Liq. Cryst.* **2003**, *404*, 15−31.

(25) Okamoto, H.; Morita, Y.; Segawa, Y.; Takenaka, S. *Mol. Cryst. Liq. Cryst.* **2005**, *439*, 2087−2093.

(26) Giamberini, M.; Reina, J. A.; Ronda, J. C. *J Polym. Sci., Part A: Polym. Chem.* **2006**, *44*, 1722−1733.

(27) Aebischer, O. F.; Aebischer, A.; Donnio, B.; Alameddine, B.; Dadras, M.; Guedel, H.-U.; Guillon, D.; Jenny, T. A. *J. Mater. Chem.* **2007**, *17*, 1262−1267.

(28) (a) Bhattacharya, S.; Mandal, S. S. *Biochemistry* **1998**, *37*, 7764−7777. (b) Bhattacharya, S.; Mandal, S. S. *Biochim. Biophys. Acta Biomem.* **1997**, *1323*, 29−44.

(29) Ghosh, Y. K.; Visweswariah, S. S.; Bhattacharya, S. *FEBS Lett.* **2000**, *473*, 341−344.

(30) Dileep, P. V.; Antony, A.; Bhattacharya, S. *FEBS Lett.* **2001**, *509*, 327−331.

(31) Ghosh, Y. K.; Visweswariah, S. S.; Bhattacharya, S. *Bioconjugate Chem.* **2002**, *13*, 378−384.

(32) (a) Bhattacharya, S.; Dileep, P. V. *J. Phys. Chem. B* **2003**, *107*, 3719−3725. (b) Bhattacharya, S.; Dileep, P. V. *Bioconjugate Chem.* **2004**, *15*, 508−519.

(33) (a) Bhattacharya, S.; Haldar, S. *Langmuir*, **1995**, *11*, 4748−4757. (b) Bhattacharya, S.; Haldar, S. *Biochim. Biophys. Acta Biomem.* **1996**, *1283*, 21−30. (c) Bhattacharya, S.; Haldar, S. *Biochim. Biophys. Acta Biomem.* **2000**, *1467*, 39−53.

(34) Bajaj, A.; Kondiah, P.; Bhattacharya, S. *J. Med. Chem.* **2007**, *50*, 2432−2442.

(35) Bajaj, A.; Kondaiah, P.; Bhattacharya, S. *Bioconjugate Chem.* **2007**, *18*, 1537−1546.

(36) Marsh, D. *Chem. Phys. Lipids* **1991**, *57*, 109−120.

(37) De, S.; Aswal, V. K.; Goyal, P. S.; Bhattacharya, S. *J. Phys. Chem. B* **1998**, *102*, 6152−6160.

(38) Weber, G.; Davis, F. J. *Biochemistry* **1979**, *18*, 3075−3078.

(39) Lakowicz, J. R.; Bevan, D. R.; Maliwal, B. P.; Cherek, H.; Balter, A. *Biochemistry* **1983**, *22*, 5714−5722.

(40) Parasassi, T.; Conti, F.; Gratton, E. *Cell. Mol. Biol.* **1986**, *32*, 103−108.

(41) Parasassi, T.; Di Stefano, M.; Loiero, M.; Ravagnan, G.; Gratton, E. *Biophys. J.* **1994**, *66*, 763−768.

(42) Parasassi, T.; De Stasio, G.; Ravagnan, G.; Rusch, R. M.; Gratton, E. *Biophys. J.* **1991**, *60*, 179−189.

(43) Parasassi, T.; De Stasio, G.; d'Ubaldo, A.; Gratton, E. *Biophys. J.* **1990**, *57*, 1179−1186.

(44) Furman, I.; Geiger, H. C.; Whitten, D. G. *Langmuir* **1994**, *10*, 837−843.

(45) Seki, T.; Ichimura, K. *J. Phys. Chem.* **1990**, *94*, 3769−3775.

(46) Bajaj, A.; Paul, B.; Indi, S.S.; Kondaiah, P.; Bhattacharya, S. *Bioconjugate Chem*. **2007**, in press.

(47) Kimizuka, N.; Kawasaki, T.; Hirata, K.; Kunitake, T. *J. Am. Chem. Soc.* **1998**, *120*, 4094−4104.

(48) Kimizuka, N.; Kawasaki, T.; Kunitake, T. *J. Am. Chem. Soc.* **1993**, *115*, 4387−4388.

(49) Mabrey, S.; Sturtevant, J. M. *Proc. Natl. Acad. Sci. U.S.A.* **1976**, *73*, 3862−3866.

(50) Sturtevant, J. M. *Proc. Natl. Acad. Sci. U.S.A.* **1982**, *79*, 3963−3967.